COMITATO NAZIONALE PER L'ENERGIA NUCLEARE
Laboratori Nazionali di Frascati

LNF-74/43(R)
27 Luglio 1974

G. Bologna, B. D'Ettorre Piazzoli, F. L. Fabbri, G. Matone, P. Picchi, A. Reale, L. Satta, P. Spillantini, G. Verri, R. Visentin and A. Zallo: HADRON FRAGMENTATION AT SPS: A STUDY OF VERTEX DETECTOR, PATTERN RECOGNITION AND EVENTS RECONSTRUCTION CRITERIA.

Servizio Documentazione
dei Laboratori Nazionali di Frascati del CNEN
Casella Postale 70 - Frascati (Roma)

Laboratori Nazionali di Frascati del CNEN
Servizio Documentazione

LNF-74/43(R)
27 Luglio 1974

G. Bologna, B. D'Ettorre Piazzoli(x), F.L. Fabbri, G. Matone, P. Picchi, A. Reale, L. Satta, P. Spillantini, G. Verri, R. Visentin, A. Zallo: HADRON FRAGMENTATION AT SPS: A STUDY OF VERTEX DETECTOR. PATTERN RECOGNITION AND EVENTS RECONSTRUCTION CRITERIA.

INTRODUCTION -

In multiparticle production in hadron-hadron interactions, the inclusive studies have indicated that very important dynamical phenomena exist, but they cannot provide unambiguous explanations of them. A powerful tool for disentangling the different production mechanisms is the study of seminclusive channels, such as single or two-particle spectra inside events of given topology. This line of research was followed with good results at the ISR(1).

The italian collaboration at SPS (Istituto di Fisica dell'Università di Milano, Istituto di Fisica dell'Università di Pisa, Istituto di Fisica dell'Università di Roma, Istituto Superiore di Sanità, Laboratori Nazionali di Frascati del CNEN) has proposed the comparative study of hadronic multiparticle production in the projectile fragmentation and pionization region induced by different particles on protons and nuclei(2).

In this paper we focus our attention on how well and to what

(x) - Laboratorio Cosmo Geofisica CNR - Torino.

extent the pattern recognition for many body events in the vertex detector of the experimental apparatus is possible.

In Section 1 we describe the essential features of the proposed set-up. In section 2 we discuss the general criteria for pattern recognition and event reconstruction in the vertex detector.

The detailed pattern recognition computer program is described in section 3.

Finally in the last sections we quote the results obtained with the afore mentioned program applied to events generated with a Monte Carlo method.

1. - EXPERIMENTAL SET-UP -

The planned detector is a multiparticle spectrometer characterized by a nearly 4π coverage and by the simultaneous detection of charged particles and photons. It is designed to provide momentum resolution sufficient to detect inelastic events in a seminclusive approach as well as a high speed in the acquisition and analysis of the events.

The detector has been designed having in mind the following criteria: modularity of the detector, symmetry for negative and positive charges and quick off-line analysis of multibody events. It consists of a forward spectrometer and of a vertex detector. The forward spectrometer measures the direction, the sign of the charge and momentum of all charged particles produced in the projectile fragmentation cone and in a part of the pionization region. The vertex detector provides information on emission angle and momentum of charged particles produced in the target fragmentation region and in the remaining part of the pionization region. Photons emitted in a forward cone of half-aperture $\sim 30^{\circ}$ around the beam direction are detected, and their energy and direction are measured with adequate resolution.

The forward spectrometer (fig. 1) consists of five standard narrow gap PS beam transport magnets in which all charged particles emitted in a narrow cone around the forward direction ($\sim \pm 7^{\circ}$) are analyzed by sets of proportional chambers. The use of five magnets provides a rather uniform sharing of measured tracks among the various sets of chambers, reducing their average number to no more than ~ 3 tracks.

The vertex detector (fig. 2) consists of an array of proportional chambers positioned inside a magnet surrounding the target. The magnet (a vertical solenoid split in two parts) provides a large volume of magnetic field ($\sim$15 Kgauss), uniform to a few percent so that it acts on forward emitted high momentum particles as part of the forward spectrometer.

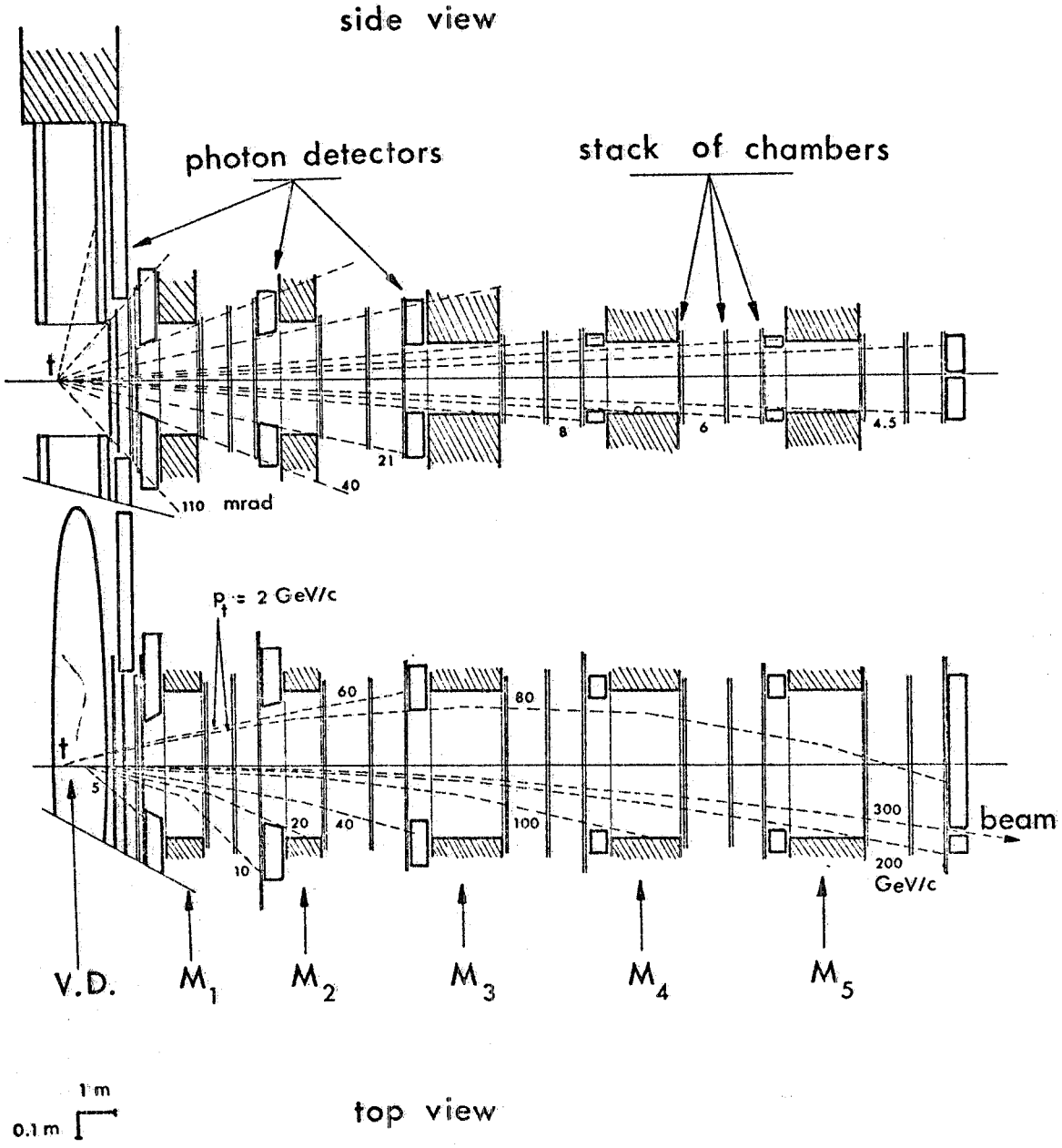

FIG. 1 - General lay-out of the experiment.

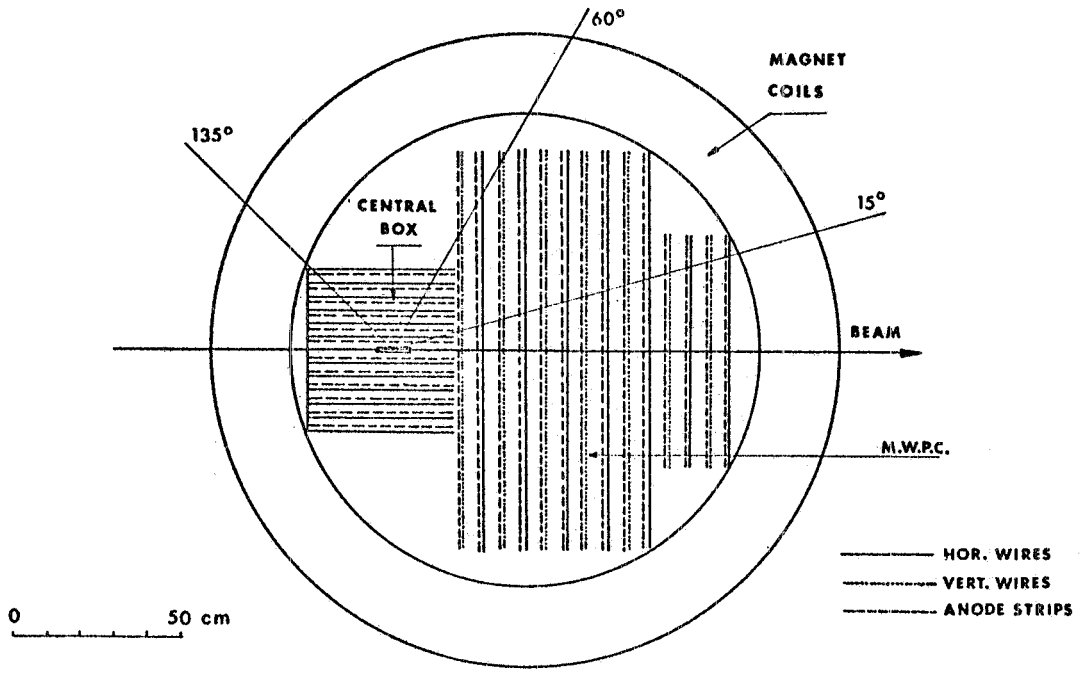

FIG. 2 - Structure of the detectors inside the vertex detector magnet. The MWPC have a rectangular shape, while CB is a set of chambers around the target.

The planned arrangement of the detectors (proportional chambers) is sketched in fig. 2. In the forward part a set of multiwire proportional chambers (MWPC) detects particles produced in a cone of $\sim 45^{\circ}$ half-aperture angle. A chamber box (CB) surrounding the target should be used to count the particles produced at very large angles, to help identifying the vertex of the event and to give a rough measurement of the particles momenta ($\Delta p/p \simeq 10\%$). We are presently considering for CB a structure of the type of MADKA i.e. a set of coaxial cylindrical chambers with wires parallel to the beam and read-out of the pulses induced on the high voltage electrodes, suitably split into helicoidal stripes[3].

2. - PATTERN RECOGNITION AND RECONSTRUCTION: GENERAL CRITERIA. -

The pattern recognization and the event reconstruction in the forward spectrometer is, in principle, easy and fast also if difficulties and errors can be introduced by multiple scattering, background, inefficiencies of chambers and other spurious effects.

The pattern recognition in the vertex detector is characterized by a large number of particles to be analized, (we have chosen $\langle n_{ch} \rangle = 6$; $(n_{ch})_{max} \simeq 20$).

Moreover most of the particles have a low momentum and large curvatures in the field. It is indeed necessary to seek for efficient simplifications of the problem, also profiting from the uniformity of the magnetic field.

In fact in a uniform field the projection of the trajectories perpendicularly to the field direction are circles so that in this plane simple and quick criteria can be found for the correct association of the measured coordinates.

The interaction point is assumed to be determined from the yz projection of the event, and can be used as an efficient constraint for the circle reconstruction.

In fact in the yz plane (containg the beam and the field direction) the trajectories are nearly straight lines(x), so that the correct association of the measured coordinates is very easy also in this plane, and the interaction point can be quickly obtained by a very simple fit procedure.

In the following sections we will explain in greater detail the outlined method for separately reconstructing the projections of tracks. For the spatial reconstruction the knowledge of a coordinate in the xy plane is needed, but a precision of an order of magnitude less than that on the yz and xz planes is sufficient. To this purpose the read out of the induced pulses on all high voltage electrodes suffices.

The association of the x and y coordinate for each point will be made quickly on line, by shifting in sequence into an AND circuit the couples of strips of the electrodes (fig. 3, 4).

3. - DESCRIPTION OF THE COMPUTER PROGRAM. -

Event generation (by MonteCarlo method), tracing in the MWPC, randomization of the read coordinates, introduction of inefficiencies and of the background, pattern recognition and event reconstruction in both xz and yz projections are performed in one computer program. The block diagram of the part for pattern recognition and the reconstruction is reported in fig. 5a) which is that used to obtain the results reported below.

The program handles separately the two projections, except for transfering to the xz projection the information on the interaction point obtained in the yz projection. Therefore also the description of the procedure and the results can be made separately. The CPU time, inclusive of event production, pattern recognition and least square fit procedure

---

(x) - Only the low momentum particles emitted at a large angle with respect to the xz plane give sinusoidal yz trajectory projections which deviate appreciably from a straight line.

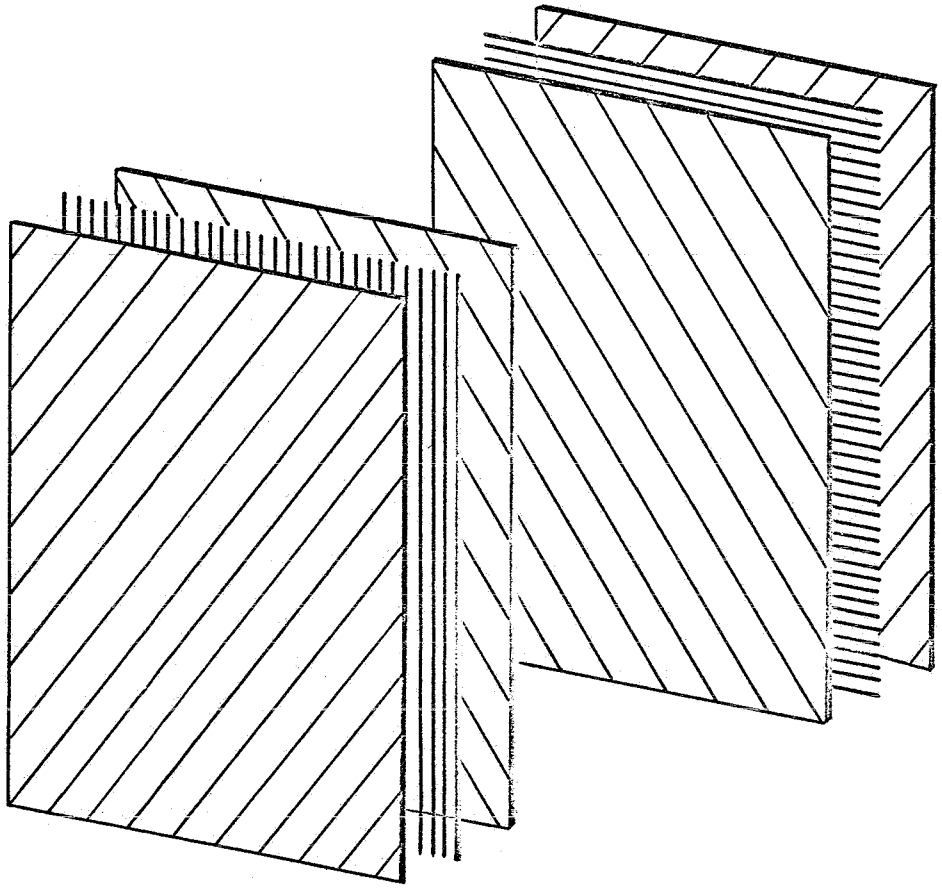

FIG. 3 - Sketch of MWPC with vertical and horizontal wires and anode strips.

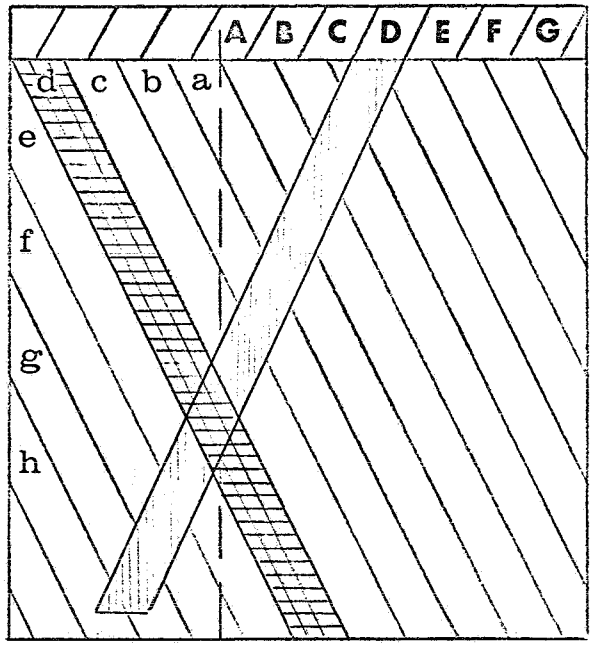

FIG. 4 - Logical criterion of sequential shifting of stripes signals into an AND circuit for spatial association of x and y coordinates.

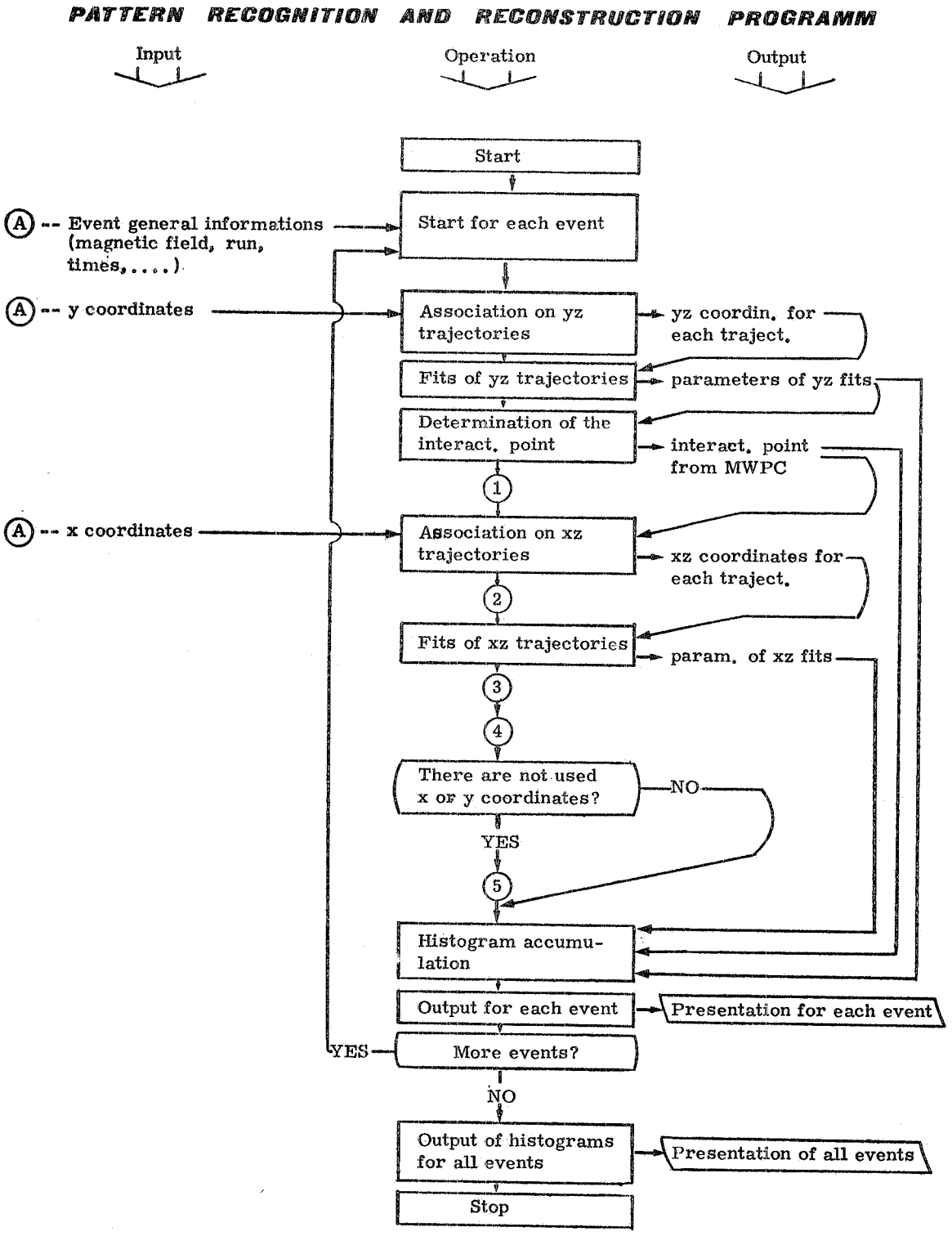

FIG. 5a - Block diagram of pattern recognition and reconstruction described in this paper.

POSSIBLE IMPLEMENTATION TO COMPLETE THE PROGRAMM

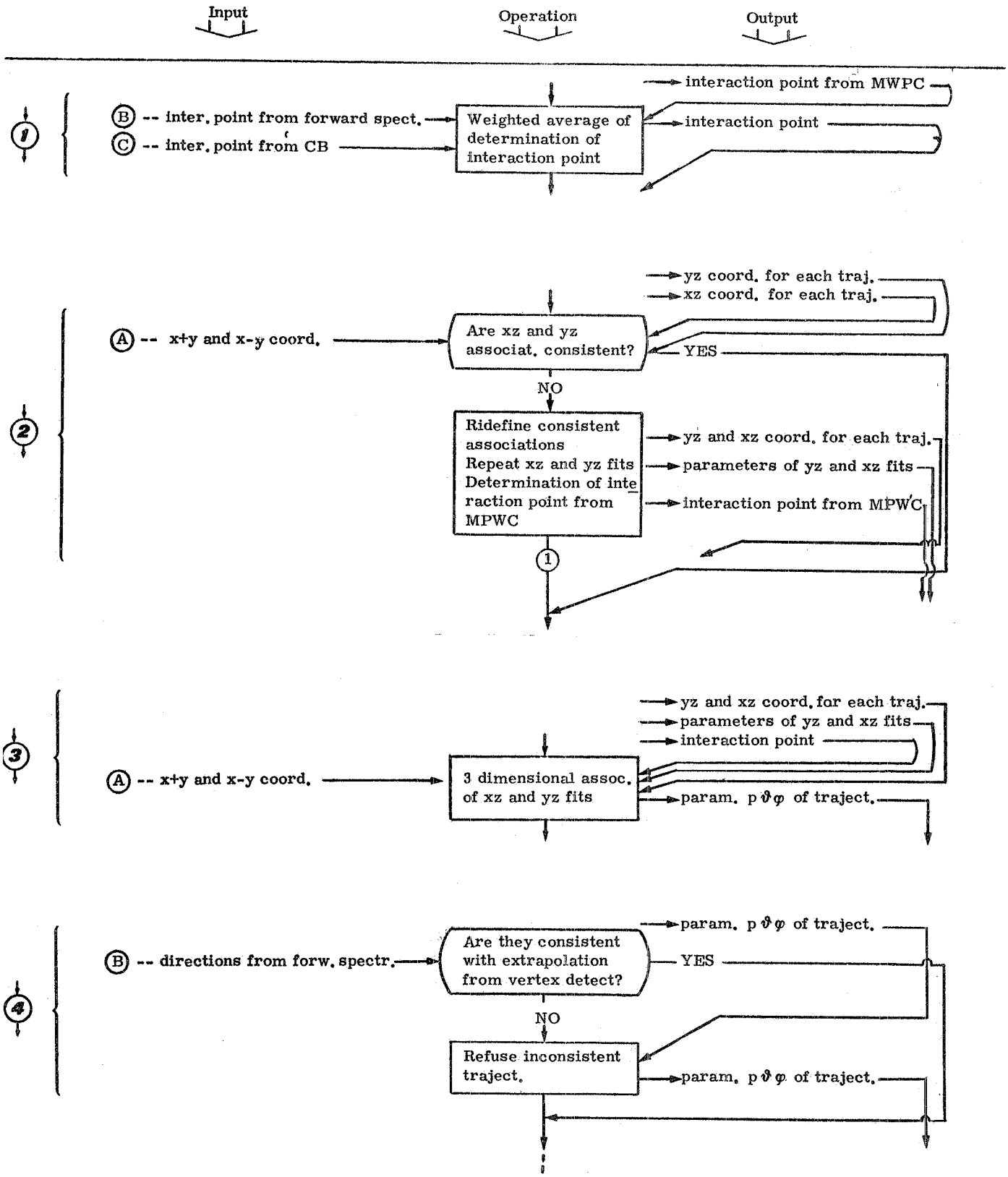

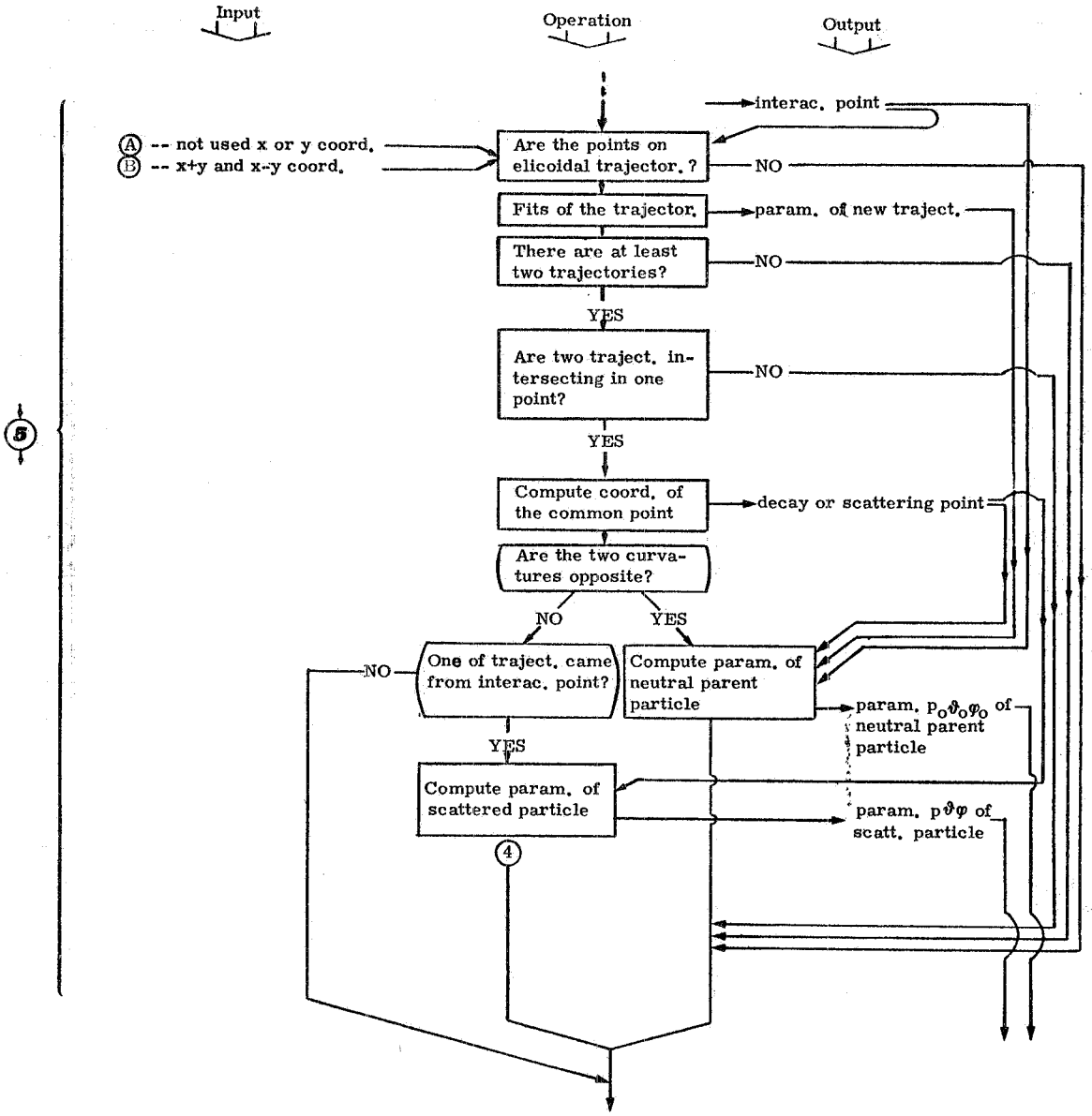

FIG. 5b - Possible implementation of the program with the following insertions :

① Determination of the interaction point from the forward spectrometer and/or the chamber box CB ;

② and ③ Exploitation of the additional x-y and x+y coordinates for the off-line consistency check between point associations in tracks in the two projections xz and yz, and for the association of the tracks measured in the two projections ;

④ Consistency check between the extrapolation of the tracks measured in the vertex detector and the tracks measured in the forward spectrometer ;

⑤ Recovery of measured coordinates not associated with a track in the first pattern recognition procedure.

averaged on all the multiplicities, is less then 0.12 sec/event of IBM system 370/165. As the computation program was written in Fortran language without any care for minimizing the time, we are confident that this time will be greatly reduced in the final version of the program.

3.1. - YZ Projection. -

Association of measured coordinates in the yz plane proceeds as indicated in fig. 6a). Starting from the coordinate y_n on the last chamber, the coordinate y_{n-1} in the (n-1) chamber is required to belong to the triangle with vertex y_n and the target as its base (fig. 7a). The coordinate y_{n-1} determines a similar requirement for the coordinate y_{n-2} on the (n-2) chamber, but with the additional condition that y_{n-2} is enclosed between the most divergent straight lines through the y_n and y_{n-1} coordinates, and so on to the y_1 coordinate. This scanning starts from the greater $|y_n|$, separately for $y_n > 0$ and $y_n < 0$. The coordinates y_1, y_2, ..., y_{n-1}, y_n which result associated on the same track are erased from the input matrix $\{y\}$, and are recorded on a special matrix $\{T_y\}$, recoverable for the analysis procedure only if in the $(n-K)^{th}$ chamber no measured coordinate is present in the scanned interval. However the pursuit of a track is not stopped if no measured coordinate is found using the $\{y\}$ and the $\{Ty\}$ matrices, what allows one to accept some inefficiency in the chambers.

If in the scanned interval two or more measured coordinates y'_{n-k}, y''_{n-k}, y'''_{n-k}, ... are found, the greater $|y_{n-k}|$ is associated with the coordinates in the previously scanned (n-k+1), (n-k+2), ... chambers.

This procedure is repeated in decreasing order of y_n for other tracks in n^{th} chamber, if any.

This pattern reconstruction is repeated for chamber (n-1), (n-2) and so on untill all chambers are exhausted.

Finally all the coordinates associated on the same track are fitted to give the z coordinate of the interaction point with its error (see point a in fig. 7a). The fitting function is simply a straight line for nearly all the tracks, and is a cubic spline only for the tracks (some percent of the total) which are most divergent from the z axis. The z coordinate of the interaction point is obtained averaging the z coordinates obtained by all the tracks of the event.

The procedure described above was used for the apparatus sketched in fig. 2, considering only MWPC spaced 12.5 cm; the error in each measured coordinate was assumed $\pm$ 1 mm, and the target length 10 cm.

We renounced the tracking of particles nearly parallel to the z-axis, and leaving the n chamber with $|y_n| < 20$ mm; in the forward spectrometer these particles go through 2 magnets and 3 sets of cham-

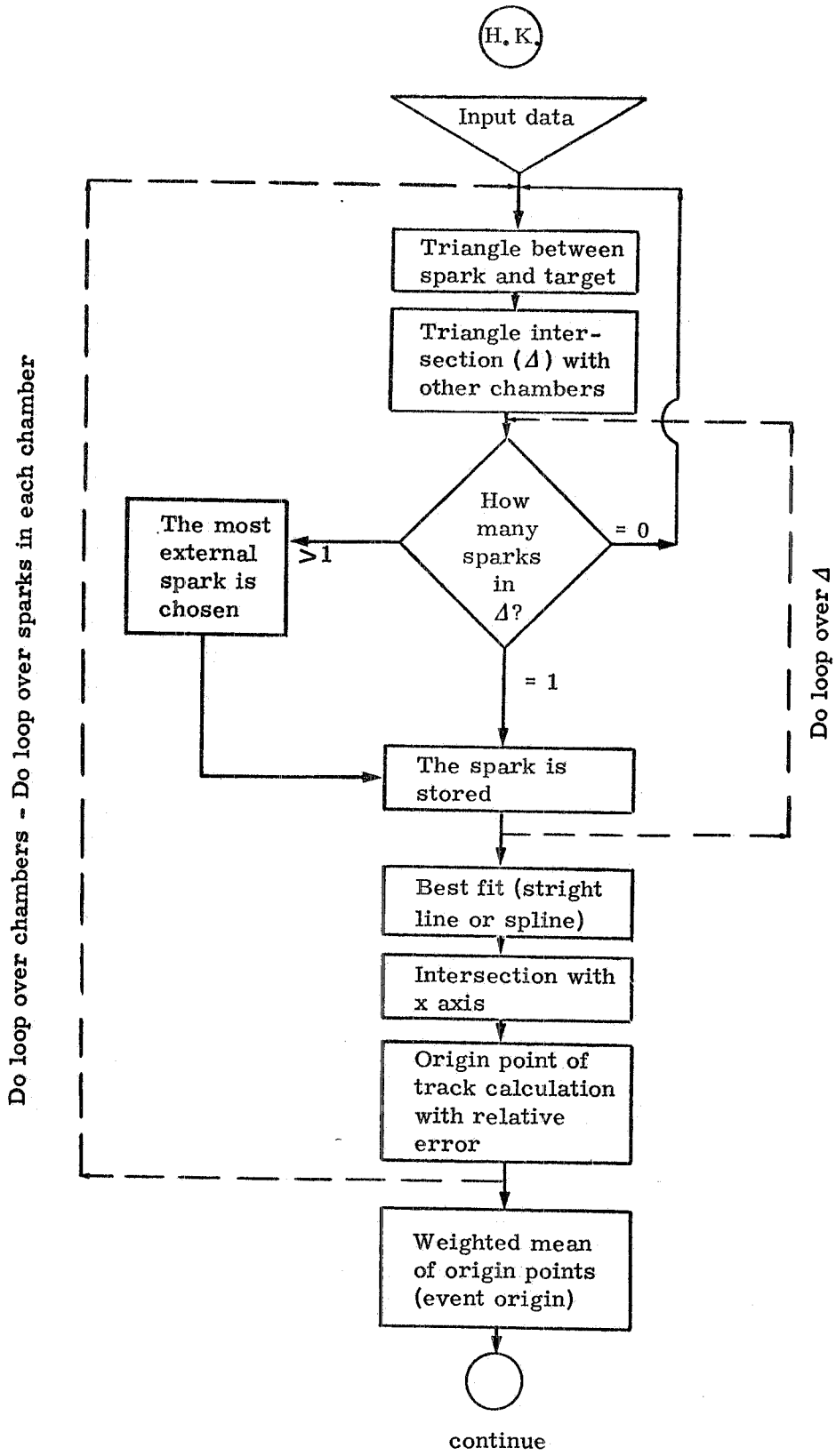

FIG. 6a - Block diagram of pattern recognition in vertical plane.

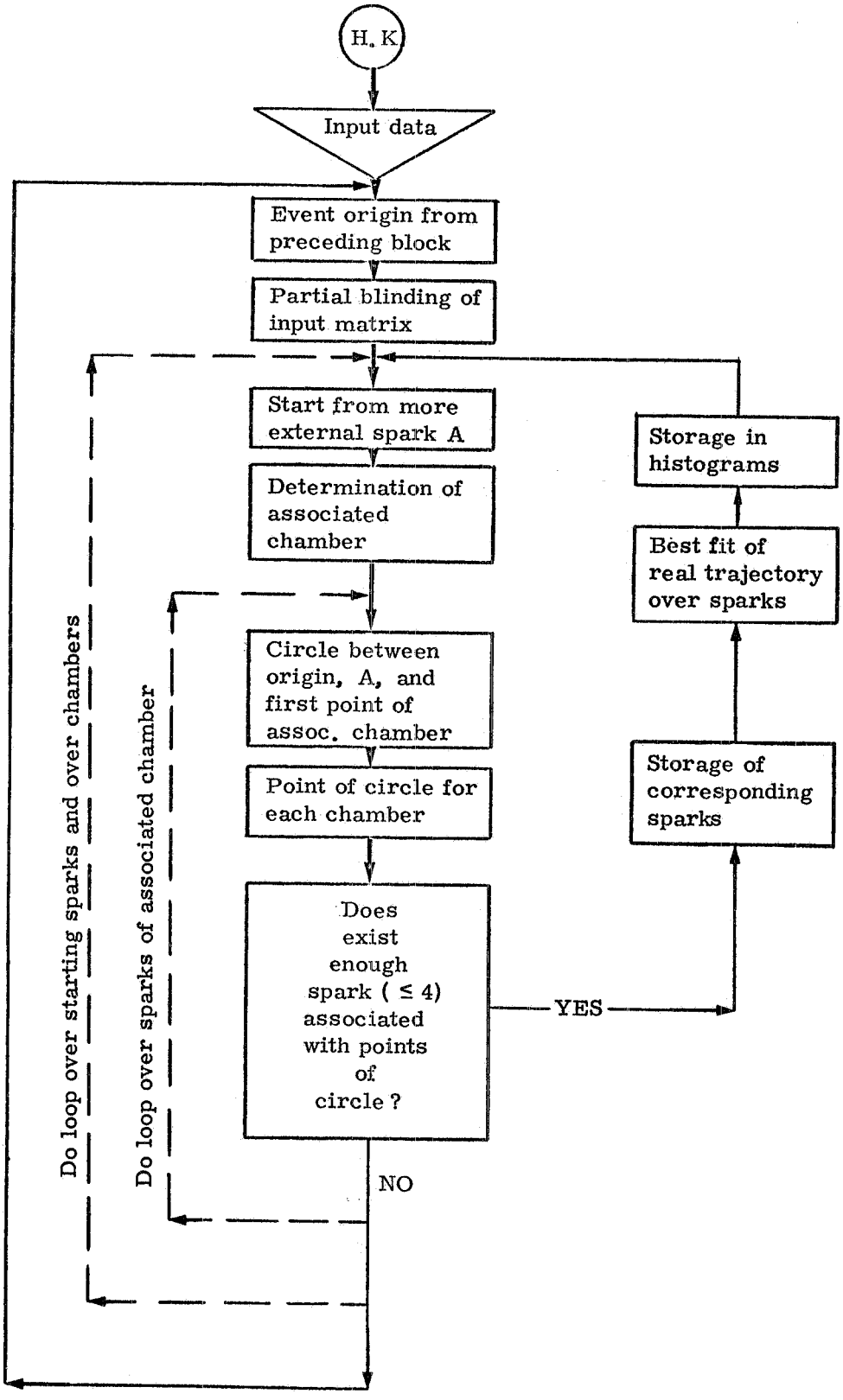

FIG. 6b - Block diagram of pattern recognition in horizontal plane.

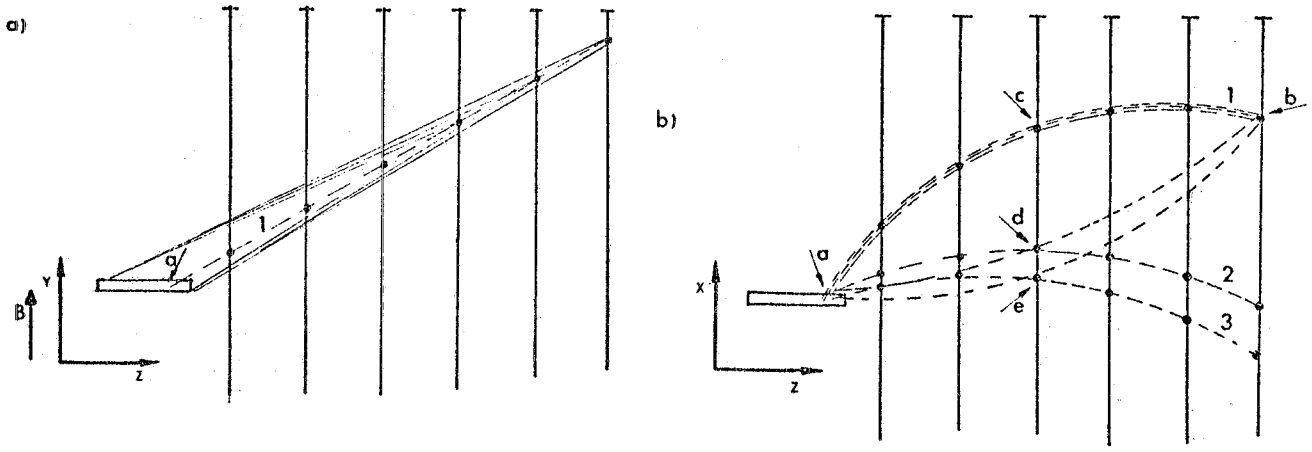

FIG. 7 - Reconstruction technique of a event in the V.D. : a) criteria to identify tracks in the vertical projected plane and determination of the interaction point (a); b) shows how starting pion points b and a the track number 1 is identified resolving the ambiguities due to points d and e in the horizontal projected plane.

bers. Indeed all particles stopping in the second forward spectrometer magnet or before can be tracked down to the target through the vertex detector.

3.2. - XZ Projection. -

The pattern recognition procedure in the xz plane is summarized in fig. 6b). Like the yz projection, the tracking starts from each x_n coordinate measured on the last chamber beginning from the most external. The association with tracks is obtained by counting how many coordinates are near to a circumference through x_n, the interaction point a (as given from the fit in the yz projection) and one of the x_k coordinates measured in the chamber of index k = n/2 (or (n+1)/2 if n is odd (see fig. 7b). This count is made for each coordinate x_k. The coordinates counted near to the same circumference, are ascribed to the same trajectory if their number is at least equal to a prefixed value, erased in the input matrix $\{x\}$ and recorded in a special matrix. A prefixed value of 2 was used allows for high inefficiencies(x) ($\sim$ 10%) in the chambers.

(x) - This was required in view of the possible substitution of the MWPC with adjustable field drift chambers, with read-out of the coordinate along the sense wire and left-right ambiguity resolution with couples of sense wires. This change would result in a considerable loss in the efficiency(4).

Having exhausted all the x_n coordinates, the procedure is repeated starting from all the x_{n-1} coordinates not yet associated with tracks, and so on.

The coordinates associated with the same track are fitted with a circumference to give the corresponding curvature with its error.

The procedure was used with 7 MWPC spaced 12.5 cm, and a $\pm$ 1 mm error on each coordinate. A region some centimeters large around the z axis ($\pm$ 2 cm in the first chamber to $\pm$ 15 cm in the last one) was considered blind, to ignore the particles that are analyzed in foward spectrometer.

4. - RESULTS -

The best value of the z-coordinate of the origin point is then calculated by averaging all values obtained in the analysis of single tracks. The spectrum of the reconstructed origin points is shown in Fig. 8 for all events and for completely reconstructed events separately. The width is of $\sim \pm 0.5$ cm.

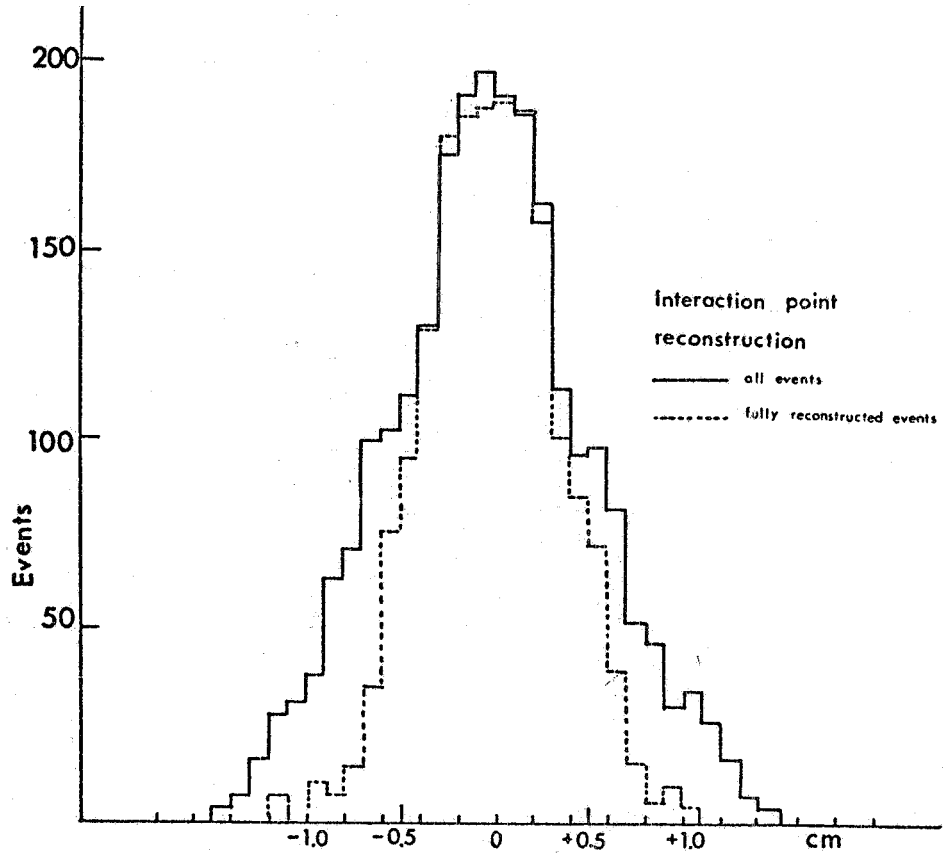

FIG. 8 - Interaction point reconstruction. In abscissa are plotted the differences between the Monte Carlo generated interaction point and the reconstructed one.

Figure 9 shows track reconstruction efficiency obtained with our program in the experimental configuration outlined above. About 90% of the tracks are correctly reproduced. Only the multiplicity in vertex detector and not the total multiplicity of the event affect the track reconstruction efficiency. The full reconstruction efficiency for what concerns the particles analyzed in the vertex detector is shown in fig. 9b). This efficiency ranges between 90% and 70% versus measured multiplicity. If we accept also events in which only one track is badly reconstructed, the efficiency varies between 100% and 90%.

The presence of spurious sparks (two per event and per chamber) in the chamber does not alter the efficiency of reconstruction. This is shown by the equality of the full curves of Figs. 9b) and 10. An inefficiency of 10% on all wires reduces, however, the percentage of reconstructed events. The $\Delta p/p$ and $\Delta \theta_{xz}$ resolutions are plotted, for various samples of events, in Figs. 11 and 12.

For each event the longitudinal and transverse component of the reconstructed momenta are summed together and compared with the same quantity calculated for the generated event in Figs. 13 and 14. For events in which no particle is lost, the average widths are $\pm$ 0.5 GeV/c in the longitudinal direction and $\pm$ 0.12 GeV/c in the transverse direction.

5. - CONCLUSIONS -

In the simplified apparatus used in the present status of the reconstruction program (i.e. no chamber box, no read out of the high voltage electrodes, no decay of unstable particles) the CPU reconstruction time is $\sim$0.1 sec/event for IBM system 360/165. This figure makes us confident that, with refinements at the language level, the on-line analysis for triggered events will be possible.

The efficiency and the resolutions with which the generated events are reconstructed are satisfactory, and will further improve when all physical informations available will be put in the program.

This calculations have been made considering the target inside the magnet. From the experimental point of view another option has been considered[2]: the positioning of the target immediately in front of the magnet.

This geometry excludes from the magnetic analysis the particles produced at an angle larger than $\sim 30^{o}$ with respect to the beam, corresponding to a region $\sim$1.5 rapidity units in the target fragmentation cone. In most of the proposed measurements the attention is focussed on the projectile fragmentation and on the central rapidity region, while in the target fragmentation cone the knowledge of the multiplicity and of the angular distribution of tracks can be sufficient.

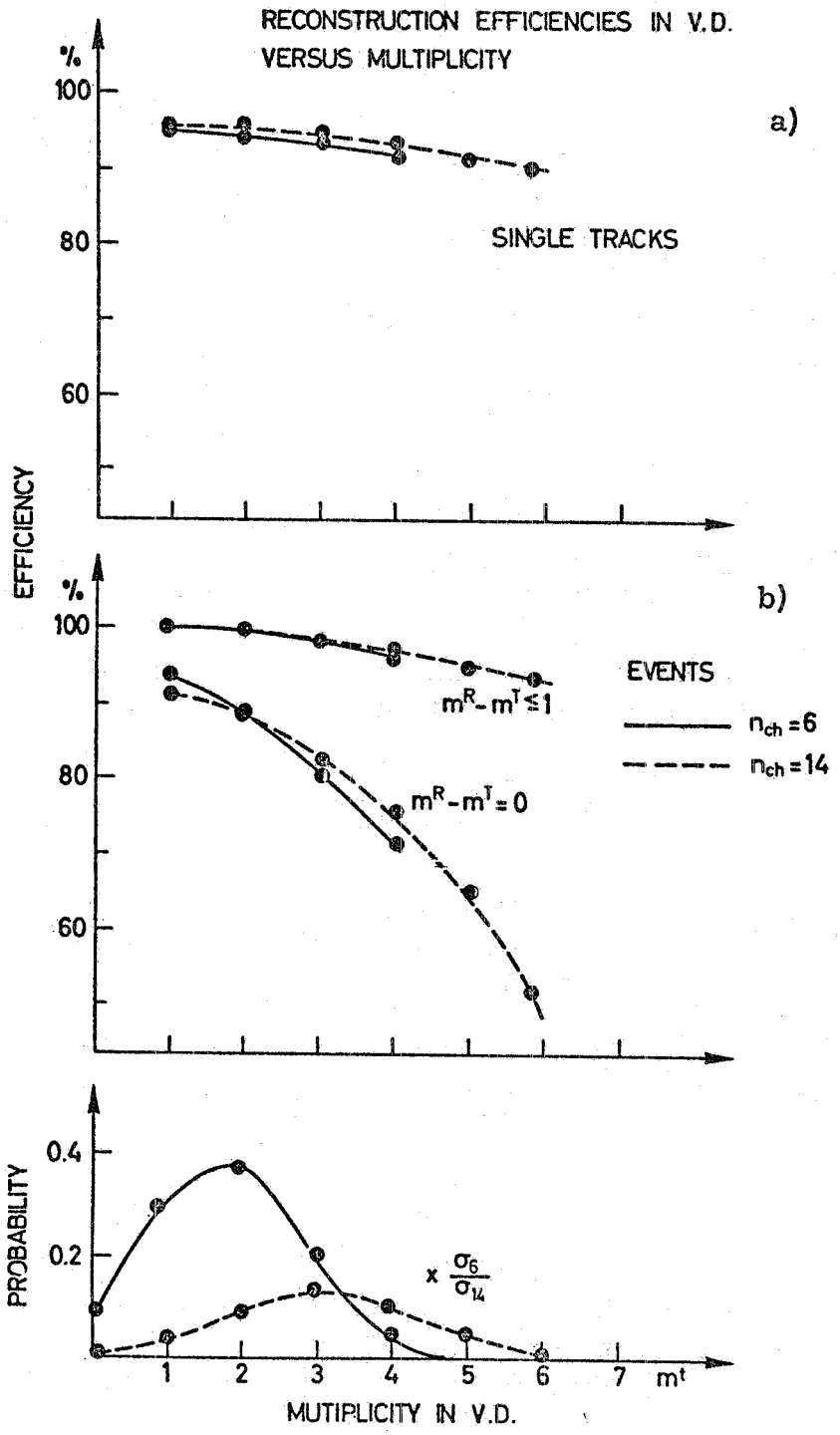

FIG. 9 - Reconstruction efficiency versus multiplicity of tracks (a) and events (b). Full line refers to events with charged multiplicity equal 6, broken line to charged multiplicity equal 14. Fully reconstructed events are indicated by $m^R - m^T = 0$. We show also the multiplicity probability in vertex detector for the two kinds of events weighted with relative cross sections.

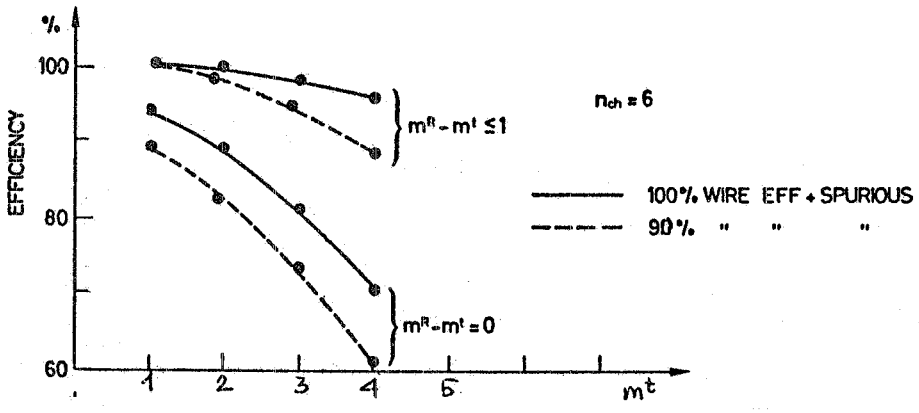

FIG. 10 - Effect of spurious sparks and wire inefficiencies on the event reconstruction efficiency for events with $n_{ch} = 6$.

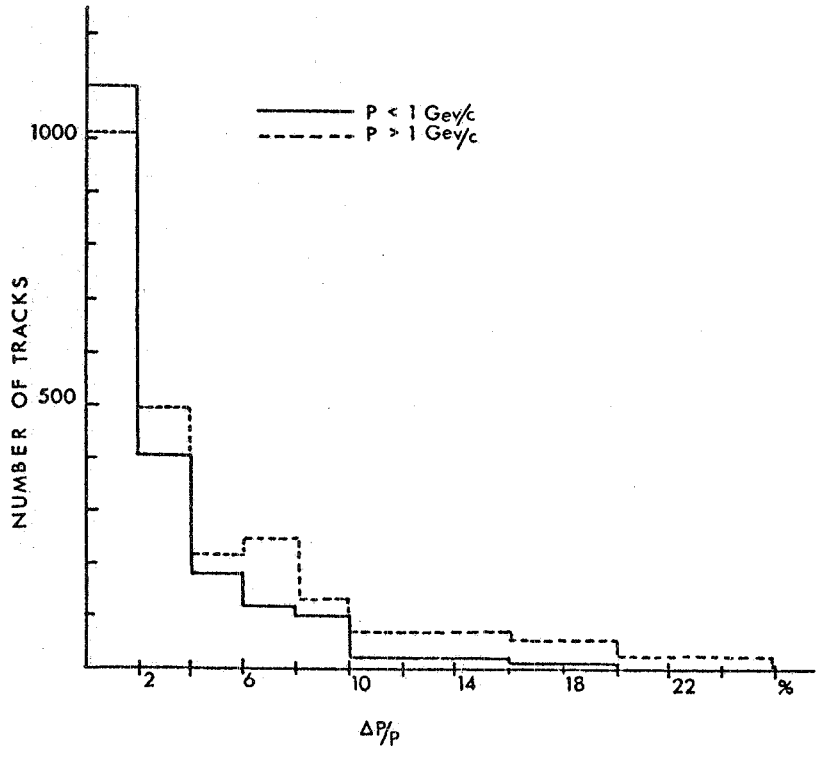

FIG. 11 - $\Delta p/p$ resolution in Vertex Detector.

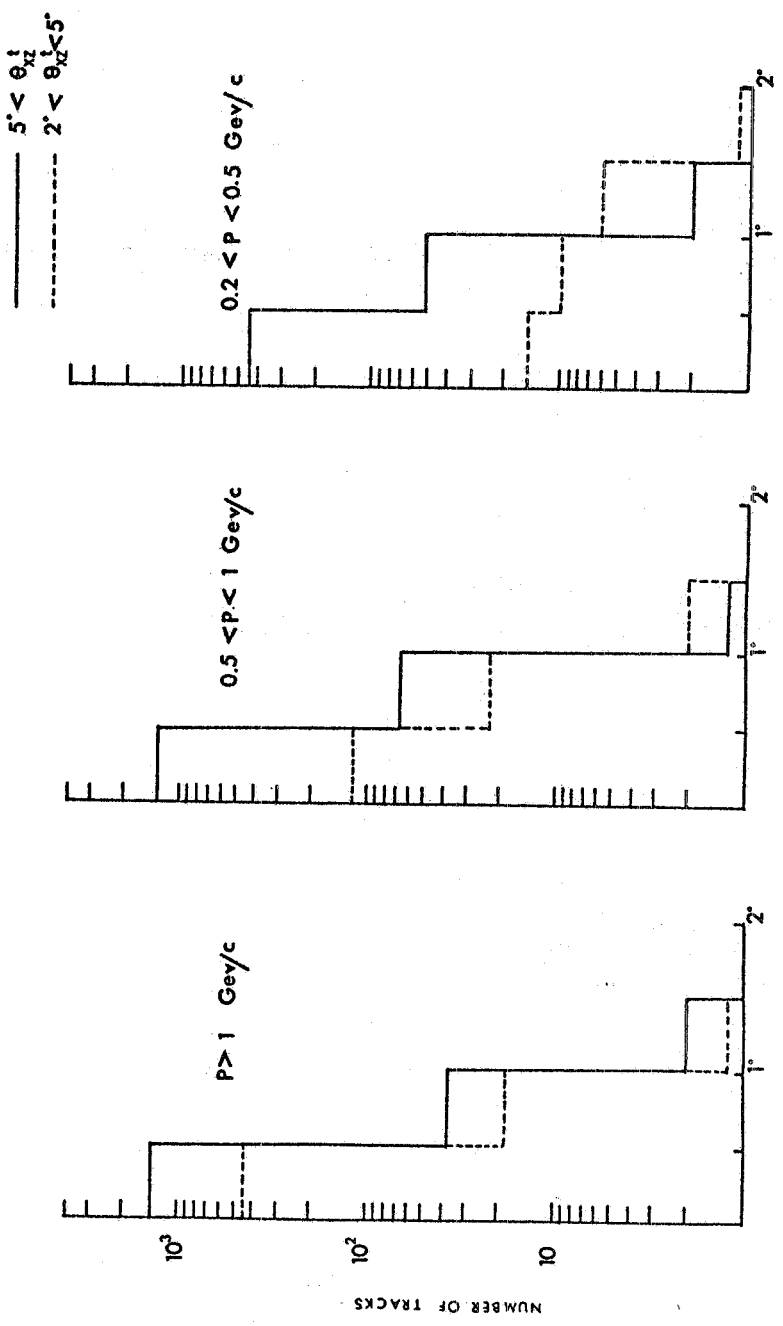

FIG. 12 - Plot of differences between the generated horizontal angle and the reconstructed one, $\Delta\theta_{xz} = | \theta^t_{xz} - \theta^r_{xz} |$, for three different ranges of particle momenta.

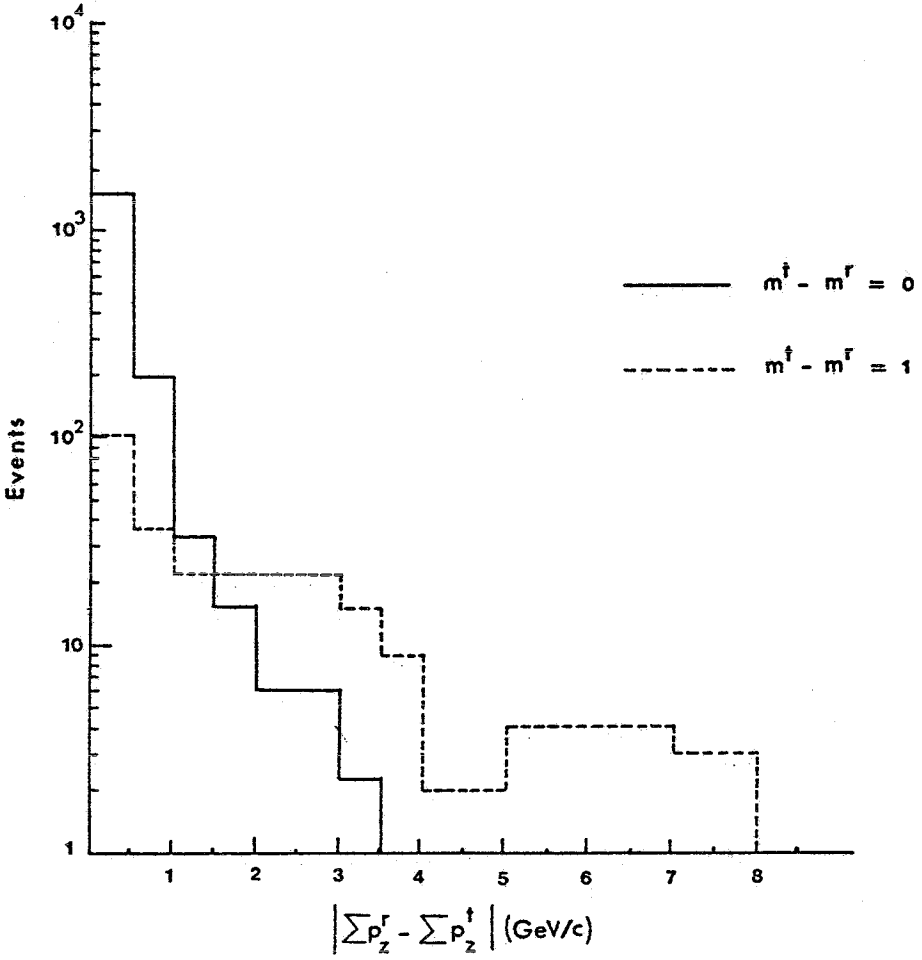

FIG. 13 - Plot of the differences between the true total longitudinal momentum and the reconstructed one of the particles of an event which are analyzed in the V.D. The full line represents fully analyzed events, the dotted line events with a missing track.

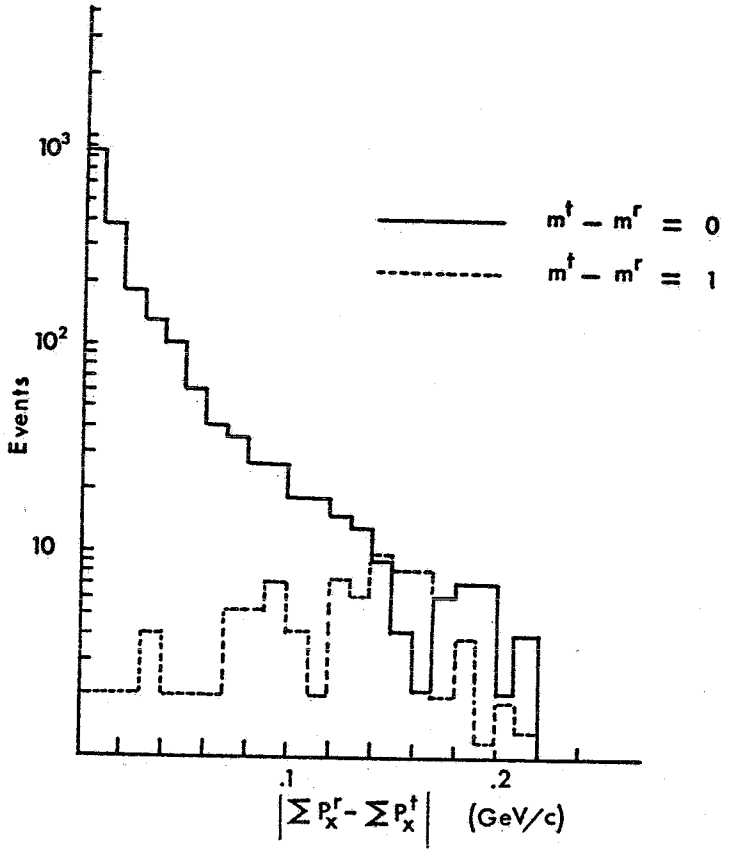

FIG. 14 - Same as Fig. 15 for transverse component of momentum.

This version of the apparatus allows us avoid the reconstruction of most difficult events (i.e., the large angle-small momentum events) inside the magnetic field.

REFERENCES -

(1) - L. Foà, Experimental Review of high multiplicity reactions, Supplement au J. de Phys. 34, C-317 (1973).
(2) - S.R. Amendolia et al., Frascati Report LNF-74/7(R) (1974), and CERN SPSC/P6 (1974).
(3) - P. Walosheck, Proc. 1973 Intern. Conf. of Instrumentation for High Energy Physics, (CNEN, Frascati, 1973), pag. 287.
(4) - A. Breskin et al., Further results on the operation of high-accuracy drift chambers, Nuclear Instr. and Meth., to be published.